Journal of Visualization, Vol. 12, No. 2 (2009) 165-172

Regular Paper

Qualitative Investigation of a Propeller Slipstream with Background Oriented Schlieren

Roosenboom, E.W.M.* and Schröder, A.*

* DLR, Institute of Aerodynamics and Flow Technology, Department Experimental Methods, Bunsenstr. 10, 37073 Göttingen, Germany.
E-mail: Eric.Roosenboom@dlr.de

Received 17 March 2008
Revised 2 October 2008

Abstract : The Background Oriented Schlieren (BOS) method has been used to qualitatively identify the (variation of) density gradients in the helical structure of a propeller slipstream. The helical structures are identified for two sideslip angles. In contrast to standard BOS correlations between exposures and a reference image, two exposures at a given time interval were cross-correlated. This revealed a more clear description of the propeller slipstream as it determines the variation of the density gradient during this interval. It enhances the visualization of the helical structure of the propeller slipstream. Based on the visualizations of the blade tip vortex trajectories the propeller slipstream contraction can be estimated.

Keywords : Propeller visualization, Vortical flow, Background Oriented Schlieren (BOS), Industrial wind tunnel

1. Introduction

It is well known that propeller-wing interactions interfere with the stability qualities and performance of a propeller aircraft (Veldhuis, 2005). Although pressure distributions on a wing can be obtained for propeller aircraft (Engler et al., 2005), limited experimental research is available that investigates these phenomena for aeronautical application. Marine propeller research is devoted to typical phenomena as wake hull interaction (Paik et al., 2007a and Felli et al., 2004) and cavitation and despite some commonalities the results are not fully transportable for the use in aerospace applications. The flow topology stemming from a rotating propeller has typical vortical structures, see for example figure 1.

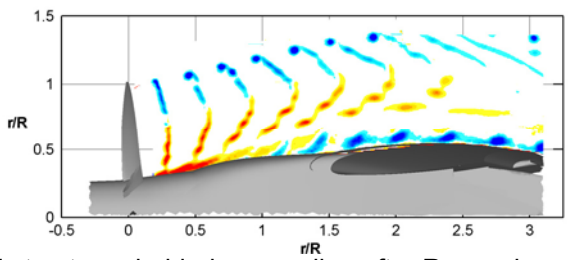

Fig. 1. Vortical structures behind a propeller, after Roosenboom et al. (2007).

In addition, the contraction of the propeller slipstream is of importance in numerical modeling of propeller flow, as the contraction alters the behavior of the flow. The Background Oriented

Schlieren (BOS) method is particularly useful for the investigation of flow structures with local density variations as present in the wakes of propeller blade tip vortices (Richard et al., 2000 and Klinge et al., 2006). The BOS method is relatively easy to set-up (Dalziel et al., 2000) and it is possible to extract 2D quantitative data from 3D flows (Venkatakrishnan et al., 2004). However, the determination of fully 3D quantitative density data requires post-processing and application of tomographic routines beyond the scope of the current investigation. The research presented in this paper aims at a qualitative visualization of the contour and the slipstream contraction behind a rotating propeller only. In the present paper the helical structures will be investigated with BOS for symmetrical conditions (no side slip, 0°) and for asymmetrical conditions (at a sideslip of 7°) for the flow behind a single-sting supported 8-bladed propeller.

2. Background Oriented Schlieren (BOS) Technique

The Background Oriented Schlieren (BOS) method relies on the relation between density gradients and the refractive index The Background Oriented Schlieren (BOS) method relies on the relation between density gradients and the refractive index (e.g. the Gladstone-Dale relation, Richard et al., 2000). Basically changes in density affect the optical path via the refractive index. The BOS method exploits this dependence by observing a random dot pattern through undisturbed and disturbed flow with CCD cameras. A simplified sketch exemplifying the main principles of the technique is presented in figure 2. The principle of the BOS technique is explained in detail in literature; see for example Richard and Raffel (2001) or Kindler et al. (2007). In a first step a randomized dot pattern is observed with cameras for an undisturbed flow without density changes in order to acquire the reference image(s). Secondly, a flow (or an object) with varying density is introduced in between the background and the cameras. Due to the varying density the optical path of the observed dots is changed and can be quantified using cross-correlation techniques similar to those in Particle Image Velocimetry (Richard et al., 2000 and Raffel et al., 2007). This results in a displacement vector field of the observed dot patterns. Based on a paraxial recording and small deflection angles the distance Δy is proportional to (Richard et al., 2000):

$$\Delta y \propto \varepsilon_y = \frac{1}{n}\int \frac{\partial n}{\partial y}\partial z \tag{1}$$

where ε_y the deflection angle, n the refractive index, y the vertical coordinate and z the horizontal coordinate. The relation between Δy and ε_y is determined by the geometric set-up of the optical system (see also figure 2). Note that the integration is along the whole optical path.

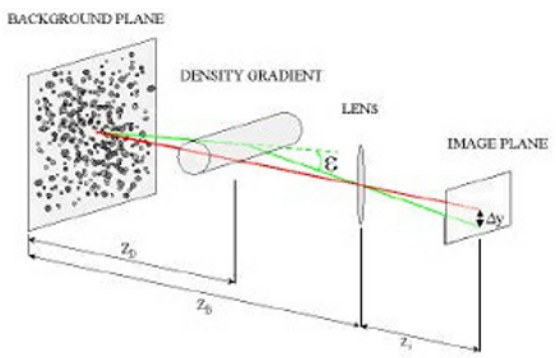

Fig. 2. Principle of the BOS technique, from Richard et al. (2000). Reprinted with permission.

The density gradient is determined by substituting the obtained refractive index calculation in the Gladstone-Dale equation. The actual density field results from the integration of the density gradient. The BOS method, thus, allows one to establish the density (gradients) in a flow. The goal of the measurements was to merely visualize the propeller slipstream, rather then determining the density itself. Therefore, in order to enhance the information observed in the slipstream two subsequent images are correlated. Effectively this determines the *variation* of the density gradient.

3. Experimental Set-up

The measurements are performed in the industrial Low Speed Wind Tunnel facility of Airbus in Bremen (Germany). The wind tunnel is an open type Eiffel wind tunnel with a contraction ratio of 4.82:1. It has a closed cross-section with an area of 2.1 m x 2.1 m. Sufficient optical access was available in this facility. Two PCO4000 CCD cameras (11 million pixels each) are used to record the images in the upper and lower half of the slipstream directly behind the propeller, see figure 3. The propeller blades rotate in clockwise sense (in pilots view). The random dot pattern has been optimized in terms of dot size and density for the high resolution of the PCO4000 cameras and the used peak-detection algorithms. It covers an area of 1.5 by 1 m^2 at the test section wall. Reference images of the background dot pattern are taken without propeller and with an idle wind tunnel. The background is illuminated with diffuse scattered pulsed laser light of a Nd:YAG laser which reduces strongly the appearance of speckle (pulse length is 9 ns). Using an advanced triggering system (Stasicki et al., 2001) linked to the propeller, double exposed images are acquired at two phase locked positions with a time interval of 100 µs. During this time interval one propeller blade rotates about 8.5° (based on a *RPM* of 14000). At the same time the convection velocity of the blade tip vortex lines leads to a half vortex tube diameter shift. This enhances the signal-to-noise ratio and doubles the measurement accuracy of the density gradient events in the slipstream. Two measurements are performed at 0° and 7° sideslip. For the sideslip angle of 7° the propeller is rotated in the horizontal plane, towards the cameras in figure 3.

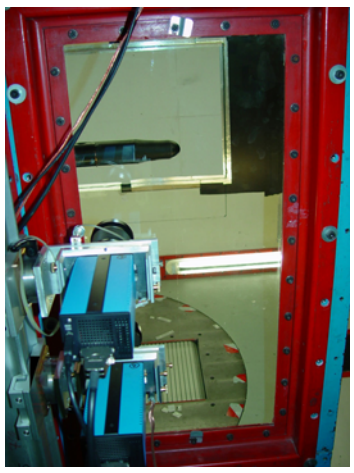

Fig. 3. Two PCO4000 CCD cameras for the BOS set-up, the BOS background is mounted at the opposite wind tunnel wall (the dots cannot be distinguished in this picture). This set-up is used for the reference images so the propeller itself is not mounted yet.

4. Results

The cross-correlation of two images acquired within a short time interval also allows neglecting random movements due to low frequency vibrations of the optical set-up. With a sufficient number of image pairs provided for averaging a very high accuracy at the determination of the sub-pixel displacement vectors has been gained. The results presented here are averaged over 200 image pairs. The change of the density gradients is obtained with a multi-grid image deformation analysis using 24 by 24 pixel final windows size and a step size of 8 pixels. Masks are generated in regions where there is no optical access due to blockage by the wind tunnel model, or at locations with significant (background) reflections.

4.1 Symmetric conditions (0° sideslip)

The BOS visualization of the slipstream for 0° sideslip is presented in figure 4(a). The displacement vectors representing the density gradients, in horizontal and vertical direction, are shown and visualized by color-coding of their magnitude. Both views of the upper and lower camera are merged into one single view. Separate masks are generated for the propeller and the nacelle regions in the upper and lower camera views and the propeller and nacelle are therefore not symmetrically masked.

The observed projection of the helical structure of the blade tip wake vortices is symmetrical. Next to the projected helical main structures, lines are running parallel. These secondary structures have a slightly lower value of magnitude and are a result from the convectional shift of the density gradient imaged at the first and second time steps. The nodal points of the slipstream projection with higher values of magnitude of the density gradients are due the integration along the whole optical path. The nodal points are a complementary effect of projecting both the 'front' and 'back' side of the slipstream. Another effect is notable in the lower part of the propeller where a region with a high variation in the density gradient is present in the near vicinity "upstream" of the propeller at about 75% of the radius. It was ensured that the mask was correctly positioned, so that mask artifacts are ruled out.

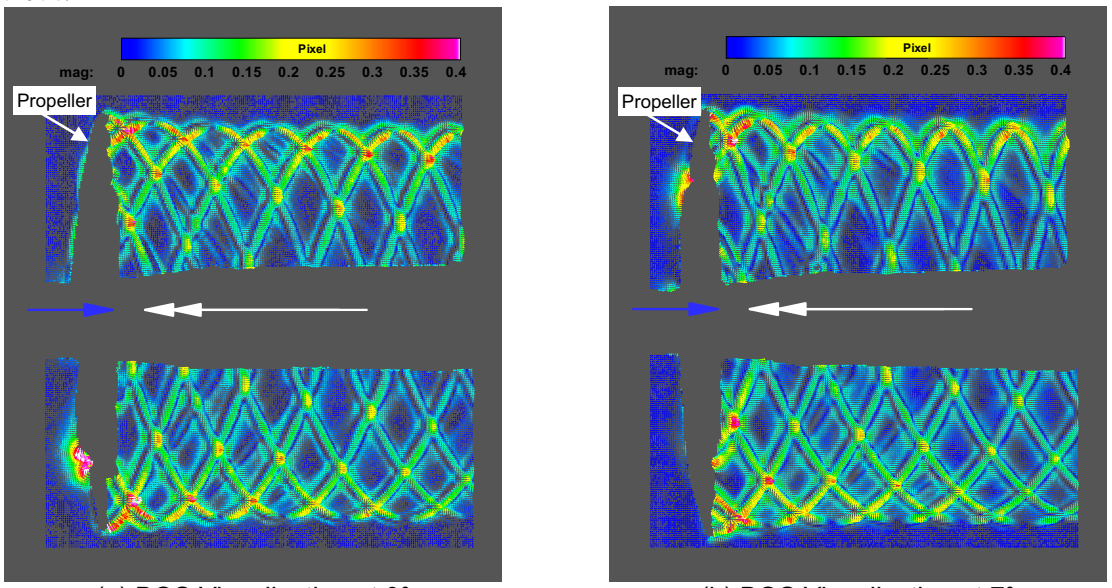

(a) BOS Visualization at 0° (b) BOS Visualization at 7°

Fig. 4. Visualizations of the helical slipstream structure at behind a rotating propeller. The direction of rotation of the propeller is indicated by the double arrow.

The density gradient close to the propeller blades at upstream position (also visible at 7° sideslip) can be explained by the pressure and density fluctuations caused by the fast moving propeller blade tips. As we use "difference" images captured at two time steps with 100 μs separation the effect is best detectable at positions where the projection direction is able to capture the change of the density gradients at the blade tip movements of 8.5° (which is not the case for the blade perpendicular to the viewing direction), where the integrating view along the blade and related density gradient is accumulating the deviation of the light path and at the same time the background dot pattern is visible for both time steps. The same measurements at the two different phase angles have been evaluated by cross-correlation with the reference image and this phenomena and temporal behavior can be confirmed.

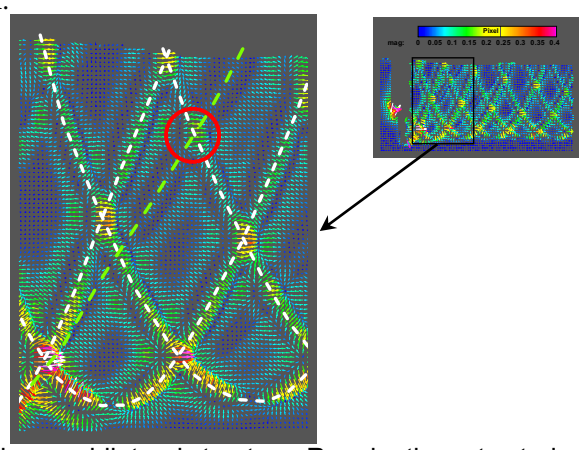

Fig. 5. Close-up of a particular quadrilateral structure. Regular tip vortex trajectories are indicated by white dotted lines, the observed extra trajectory by a green dotted line. An extra node is highlighted by the red circle.

Within the quadrilateral structures, formed by two subsequent helices, also a variation in the density gradient is present. A close-up is presented in figure 5. In fact, the BOS set-up not only determines the density gradients from the helical structure (white dotted lines), but from other sources as well. The angle of the green dotted line is more moderate than the other projected angles. It cannot be related to the change in angle during two subsequent image recording, since this would yield just a phase shift with lines running parallel. The milder angle indicates a higher convection velocity. At the wakes of each passing propeller blade shear layers are formed causing a zone of lower density. These shear layers formed at sections other than the tip region are convected faster within the slipstream, where the highest velocity increase occurs. Of course, any difference in density gradients is detected in the integrated results for the variation of the density gradient.

4.2 Asymmetric conditions (7° sideslip)

Figure 4(b) shows the BOS visualization of the propeller slipstream for 7° sideslip. The propeller is rotated horizontally towards the cameras in figure 3. The helical structure is a projected view of the helical structure at 0° and appears therefore very similar. Due to the projection the quadrilateral structure in the upper part and the lower part are different. Figure 6 compares two projections of 8 predefined helical structures. In particular, the difference between both views is present in the structures of two consecutive helices. Where these structures are symmetric for 0° case, they are different for 7°. In the upper part the structures are stretched in vertical direction and in the lower part these structures appear compressed, compare the highlighted structures in figure 6(b). The observed deviations of the structures at the edge of the slipstream are therefore due to the projection angle.

However, other differences can be observed as well. First, the density gradient variations in tip regions (in the upper and lower views) are slightly lower than for the 0° case. Of course, these lower values can also be explained by projection angle. Due to direction of rotation the distance from the propeller to the cameras is smaller than at 0° and will result in a lower value for the variation the density gradient. Again, the higher values at the nodal points are due to the complementary effect simultaneously visualizing the density gradients the 'back' and 'front' side of the propeller slipstream. Secondly, a region with higher values is now present at 2/3 of the radius in the upper view. Although at 7° sideslip it makes sense that the flow is not symmetric also for this case higher density gradients observed in the flow field upstream of the propeller. But as opposed to the 0° case, this region is now in region of the propeller. This area can however be explained by the same reasoning as for the 0° case, namely combination of the view and the accumulation of gradients due to the integration along the optical path.

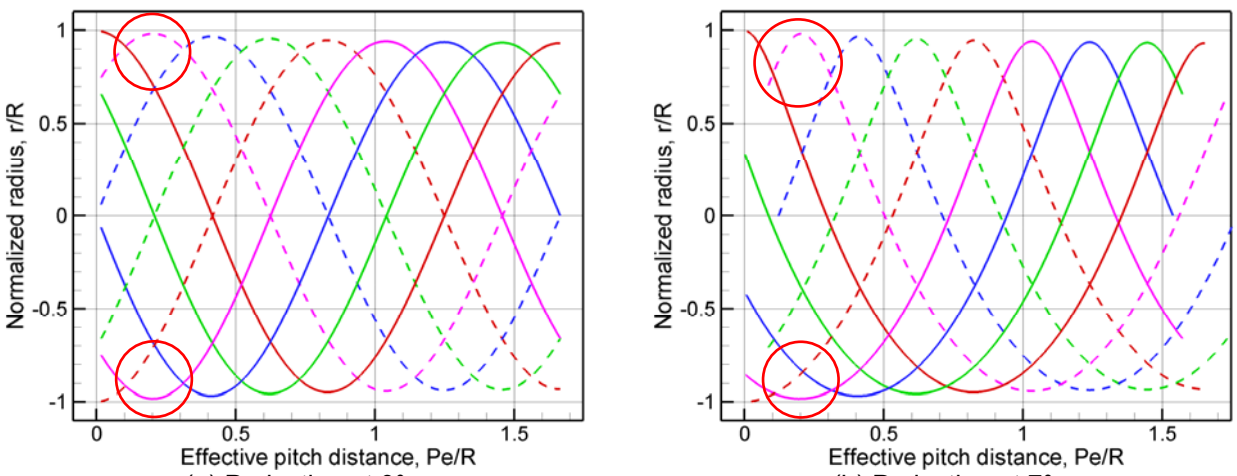

(a) Projection at 0° (b) Projection at 7°

Fig. 6. Projection of helical structure of 8 tip vortices for 1 revolution, with slipstream contraction. Typical differences due to the projection are highlighted with red circles.

4.3 Determination of slipstream contraction

The effective pitch is defined as the distance the propeller 'travels' per revolution and is readily obtained by equation (2), where U_∞ is the free stream velocity and n_p the number of revolutions per

second.

$$Pe = U_\infty / n_p \tag{2}$$

A helix has a constant radius for every revolution and is given by the following parametric equations for the x, y and z-coordinates, see also figure 7 for a graphical representation:

$$\begin{aligned} &x = Rs\cos\theta, \quad y = Rs\sin\theta, \quad z = c\theta \\ &\text{with } \theta \in [0, 2\pi] \end{aligned} \tag{3}$$

where Rs is the radius of the disk spanned by x and y, θ the angle of the revolution of the helix and c a constant defined as $c = Pe/2\pi$.

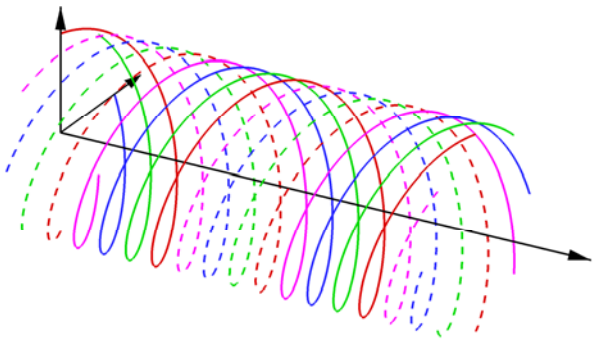

Fig. 7. Representation of 8 helices.

Due to the velocity increase at the propeller disk the fluid is accelerated and as a result the slipstream will contract in order to conserve mass flow. This slipstream contraction geometry is needed for wake modeling in computational fluid dynamics and cannot be neglected for highly loaded propellers since the effective angle of attack of a wing in a propeller slipstream is altered (Veldhuis, 2005). Providing experimental insight of the slipstream contraction will also enable a more realistic wake modeling (Paik et al., 2007b). The current BOS set-up is focused on the slipstream visualization of a single-sting mounted propeller. This set-up can easily be extended to study the effects of propeller wing interaction for a propeller-wing model. In combination with (dynamic) balance measurements this would give great insight in the propeller-wing interaction phenomena and can be evaluated with an appropriate BOS set-up.

Figure 6(a) shows the projected structure of a contracted helix. The horizontal axis represents the effective itch distance, as given by equation (2). This contraction factor is determined according to equation proposed by Veldhuis (2005, Appendix C). The equation is derived for a flow without a nacelle and assumes an actuator disc with uniform axial force distribution. The slipstream contraction equation is given in equation (4). The slipstream contraction depends mainly on the thrust (coefficient) and the distance, z, behind the propeller disc. A qualitative comparison with the observed slipstream contraction in figures 4(a) and (b) reveals that the slipstream contracts within a shorter distance behind the propeller than is estimated with the contraction formula given in equation (4). Indeed, the presence of the sting reduces the effective flow area, which contributes to an additional velocity increase. As a result the slipstream will contract stronger.

$$Rs = R\sqrt{\frac{1+a}{1+a\left(1+\frac{z}{\sqrt{R^2+z^2}}\right)}} \tag{4}$$

The constant a is the axial inflow factor and follows from the axial momentum theory of propellers, e.g. the tangential velocity component is neglected:

$$a = \tfrac{1}{2}\left(-1+\sqrt{1+\tfrac{8}{\pi}T_c}\right) \tag{5}$$

The thrust coefficient, T_c, is defined as:

$$T_c = \frac{T}{\rho V_\infty^2 D^2} \tag{6}$$

where T is the thrust, the density, V_∞ the free stream velocity and D the diameter of the propeller.

Appropriate values are substituted in the graphical representation of the contracted helices in figure 6. The measurements were merely performed to establish the readiness and applicability of the BOS method to this type of flow, so the actual distances of the optical set-up are not measured. Nevertheless, valuable information can be in principle obtained by estimating the slipstream contraction based on an appropriate BOS visualization. Based on the current observations with nacelle it seems plausible that a correction factor for the formula for the slipstream contraction in equation (4) can be provided. Such information will improve the wake modeling in computational fluid dynamics.

5. Conclusions

The helical structure of the trailing tip vortex trajectories behind a rotating propeller was investigated qualitatively using the Background Oriented Schlieren (BOS) method. Similar to PIV correlations, two subsequent images are correlated with each other. The presented results therefore are an estimate of the *variation* of the density gradient. Only qualitative results are presented. The measurements were performed at two sideslip angles of 0° and 7°. The structures in the slipstream compare very well to theoretical projections of helical structures. The slipstream contraction can readily be obtained with the current visualization technique. Comparison with a slipstream contraction formula indicates that for a correct wake modeling in CFD a detailed description of the slipstream contraction geometry is needed. A possible extension for further measurements could be a simultaneous measurement of the slipstream and the handling qualities of the full- or half-model propeller aircraft. This will allow an immediate feedback of the connection between aircraft stability and propeller-wing interference. For the case of a rotating flow it could be beneficial to perform several measurements at several different phase angles. In particular the effects of the observed variation of the density gradient could be addressed with such a measurement. Additionally, a tomographic reconstruction of the propeller slipstream can be performed if sufficient views at multiple phase angles are available.

Acknowledgment

The measurement campaign was performed as part of close collaboration project work on behalf of Airbus. This project was conducted within the German IHK-HICON research program and is funded by the German Ministry for Economics and Labor. This paper has been presented as number #274 at the ISFV13 Conference.

References

Dalziel, S.B., Hughes, G.O. and Sutherland, B.R., Whole-field measurements by 'synthetic schlieren', Experiments in Fluids 28, 322-335, 2000.

Engler, R.H., Fey, U., Klein, Chr. and Sachs, W.E., Quantitative Wind Tunnel Studies Using Pressure- and Temperature Sensitive Paints, Journal of Visualization (8) 3, 277-284, 2005.

Felli, M. and Di Felice, F., Analysis of the Propeller-hull Interaction by LDV Phase Sampling Techniques, Journal of Visualization (7) 1, 77-84, 2004.

Kindler, K., Goldhahn, E., Leopold, F. and Raffel, M., Recent developments in background oriented Schlieren methods for rotor blade tip vortex measurements, Experiments in Fluids 43 (2-3), 233-240, 2007.

Klinge, F., Raffel, M., Hecklau, M., Kompenhans, J. and Göhmann, U., Measurement of the position of rotor blade vortices generated by a helicopter in free-flight by means of the stereoscopic Background Oriented Schlieren Method (BOS), 13th International Symposium on Application of Laser Techniques to Fluid Mechanics, Lisbon, Portugal, June 26-29, 2006.

Raffel, M., Willert, C.E., Wereley, S.T. and Kompenhans, J., Particle Image Velocimetry: A practical guide (2nd edition),

Springer-Verlag, Berlin Heidelberg, 2007.
Paik, B.-G., Kim, G.D., Lee, J.Y., and Lee, S.J., Visualization of the Inflow Ahead of a Rotating Propeller attached to a Container Ship Model, Journal of Visualization (10) 1, 47-55, 2007a.
Paik, B.-G., Kim, J., Park, Y.-H., Kim, K.-S. and Yu, K.-K., Analysis of wake behind a rotating propeller using PIV technique in a cavitation tunnel, Ocean Engineering 34, 594-604, 2007b.
Richard, H., Raffel, M., Rein, M., Kompenhans, J. and Meier, G.E.A., Demonstration of the applicability of a Background Oriented Schlieren (BOS) method, 10th International Symposium on Applications of Laser Techniques to Fluid Mechanics, Lisbon, Portugal, July 10-13, 2000.
Richard, H. and Raffel, M., Principle and applications of the background oriented schlieren (BOS) method, Measurement, Science and Technology 12, 1576-1585, 2001.
Roosenboom, E.W.M., Heider, A. and Schröder, A., Propeller Slipstream Development, 25th AIAA Applied Aerodynamics Conference, Miami, FL, June 25-27, 2007.
Stasicki, B., Ehrenfried, K., Dieterle, L., Ludwikowski, L. and Raffel, M., Advanced synchronization techniques for complex flow field investigations by means of PIV (Paper 1188), Proceedings of the 4th International Symposium on PIV, Göttingen, Germany, September 17-19, 2001.
Veldhuis, L.M.M., Propeller wing aerodynamic interference, PhD Thesis, Delft University Press, Delft, 2005.
Venkatakrishnan, L. and Meier, G.E.A., Density measurements using the Background Oriented Schlieren technique, Experiments in Fluids (37), 237-247, 2004.

Author Profile

Eric W.M. Roosenboom: He received his B.Sc. (2003) and M.Sc. in Aerospace Engineering (2005) from the Delft University of Technology. He worked shortly in the Aerodynamics department at the faculty of Aerospace Engineering in 2005. Since 2006 he is employed by DLR (German Aerospace Center) as a research scientist, in a partnership with Airbus Germany. His research interests are (experimental) aerodynamics, PIV, BOS, unsteady flow phenomena, flow statistics, coherent structures and propeller flow.

Andreas Schröder: He received his diploma degree in physics in 1996 and his PhD degree (Dr. rer. nat.) in 2001 from the Univ. of Göttingen. Since 1997 he works as a research scientist at DLR (German Aerospace Center) in Göttingen with special emphasis on the application of PIV and 3D PIV to turbulent and transitional boundary layers and in project leader position for several research and industry projects using Stereo PIV and BOS techniques in aerodynamic testing in industrial wind tunnels. He is organizer of the annual international PIV Course at the DLR in Göttingen, 2002 -2008 (http://pivcourse.dlr.de) and was coordinator of EC funded the thematic network Particle Image Velocimetry “PivNet 2” (38 partners) from May 2004 to December 2008 (http://pivnet.dlr.de).